DOI: 10.1021/ic901219f

Inorganic Chemistry
Article

Syntheses, Structures, and Magnetic Properties of Tetramanganese(III) and Hexamanganese(III) Complexes Containing Derivative of Biguanidate Ligand: Ferromagnetic Interaction via Imino Nitrogen

Asako Igashira-Kamiyama,*,† Takashi Kajiwara,*,‡,§ Motohiro Nakano,∥ Takumi Konno,† and Tasuku Ito§

†*Department of Chemistry, Graduate School of Science, Osaka University, Toyonaka, Osaka 560-0043, Japan,* ‡*Department of Chemistry, Faculty of Science, Nara Women's University, Nara 630-8506, Japan,* §*Department of Chemistry, Graduate School of Science, Tohoku University, Aoba-ku, Sendai 980-8578, Japan, and* ∥*Department of Applied Chemistry, Graduate School of Engineering, Osaka University, Suita, Osaka 565-0871, Japan*

Received June 25, 2009

The tetramanganese(III) and hexamanganese(III) complexes, $[Mn_4(\mu\text{-pzbg})_2(Hpzbg)_2(MeO)_4(MeOH)(H_2O)]Cl_2$ (**1**) and $[Mn_6O_4(Hpzbg)_4(AcO)_4(MeO)_2]$ (**2**), were synthesized by using a monopyrazolyl biguanide derivative (H_2pzbg) as a multinucleating ligand, which was newly prepared by the nucleophilic addition of pyrazole to Dicyandiamide. Single-crystal X-ray analysis revealed that **2** possesses a face-sharing double cubane structure, in which six Mn(III) ions are bridged by six MeO^- with four terminal κ^2N-Hpzbg$^-$. On the other hand, **1** possesses an incomplete face-sharing double cubane structure in which four Mn(III) ions are bridged by four MeO^- and two $\kappa^2N{:}\kappa^2N$-pzbg^{2-} accompanied by two terminal κ^2N-Hpzbg$^-$. In **1**, both ferromagnetic and antiferromagnetic interactions occur between manganese(III) ions, of which the ferromagnetic one is assigned to be the interaction via the imino nitrogen atom, while all manganese(III) ions are connected in an antiferromagnetic manner in **2**.

Introduction

Polynuclear 3d metal complexes have attracted considerable attention in a vast range of fields including models for bioinorganic chemistry and their intriguing physical and chemical properties such as magnetic, electronic, and catalytic properties.[1−4] To explore and to control these properties, it is important to design their structures by using either well-organized organic ligands or complex ligands.[5,6] Along this line, we have been creating a new ligand system based on biguanide derivatives (Figure 1a, Hpz_2bg), which leads to the formation of well-organized polynuclear metal clusters. Previously, we have shown that this ligand system possesses ferromagnetic interaction pathways achieved by the control of bridging geometries.[7−9] When two metal ions having dσ spins were bridged by this type of ligand in a $\kappa^1N{:}\kappa^2N$ or $\kappa^1N{:}\kappa^2O$ mode, the orthogonality of two metal $d_{x^2-y^2}$ orbitals afforded a ferromagnetic interaction between metal centers. The trinuclear complexes constructed from the complex ligand $[Cu(pz_2bg)_2]$ with a $\kappa^3N{:}\kappa^2N$ bridging manner showed the ferromagnetic interactions between Cu(II) and M(II) ions (M = Cu, Ni, Co, and Mn). This result indicated that the

*To whom correspondence should be addressed. E-mail: igashira@chem.sci.osaka-u.ac.jp (A.I.K.); kajiwara@cc.nara-wu.ac.jp (T.K.).

(1) (a) Singleton, M. L.; Bhuvanesh, N.; Reibenspies, J. H.; Darensbourg, M. Y. *Angew. Chem., Int. Ed.* **2008**, *47*, 9492. (b) Kruppa, M.; Knig, B. *Chem. Rev.* **2006**, *106*, 3520.

(2) (a) Pardo, E.; Ruiz-García, R.; Cano, J.; Ottenwaelder, X.; Lescouëzec, R.; Journaux, Y.; Lloret, F.; Julve, M. *Dalton Trans.* **2008**, 2780. (b) Gatteschi, D.; Sessoli, R. *Angew. Chem., Int. Ed.* **2003**, *42*, 268. (c) Miller, J. S.; Drillon, M. *Magnetism: Molecules to Materials III*; Wiley-VCH: Weinheim, 2002.

(3) Huynh, M. H.; Meyer, T. *J. Chem. Rev.* **2007**, *107*, 5004.

(4) (a) Rach, S. F.; Kühn, F. E. *Chem. Rev.* **2009**, *109*, 2061. (b) Punniyamurthy, T.; Velusamy, S.; Iqbal, J. *Chem. Rev.* **2005**, *105*, 2329.

(5) (a) Saalfrank, R. W; Maid, H.; Scheurer, A. *Angew. Chem., Int. Ed.* **2008**, *47*, 8794. (b) Dalgarno, S. J.; Power, N. P.; Atwood, J. L. *Coord. Chem. Rev.* **2008**, *252*, 825.

(6) (a) Kitagawa, S.; Noro, S.; Nakamura, T. *Chem. Commun.* **2006**, 701. (b) Halper, S. R.; Do, L.; Stork, J. R.; Cohen, S. M. *J. Am. Chem. Soc.* **2006**, *128*, 15255.

(7) (a) Igashira-Kamiyama, A.; Kajiwara, T.; Konno, T.; Ito, T. *Inorg. Chem.* **2006**, *45*, 6460. (b) Kamiyama, A.; Kajiwara, T.; Yamaguchi, T.; Ito, T. *Abstracts of Papers*; 39th IUPAC Congress and 86th Conference of the Canadian Society for Chemistry; Ottawa, Canada, **2003**. (c) Kamiyama, A.; Kajiwara, T.; Ito, T. *Abstracts of Papers*; 35th International Conference on Coordination Chemistry; University of Heidelberg, Heidelberg, Germany, **2002**.

(8) (a) Kajiwara, T.; Kamiyama, A.; Ito, T. *Chem. Commun.* **2002**, 1256. (b) Kajiwara, T.; Kamiyama, A.; Ito, T. *Polyhedron* **2003**, *22*, 1789.

(9) (a) Kamiyama, A.; Noguchi, T.; Kajiwara, T.; Ito, T. *CrystEngComm* **2003**, *5*, 231. (b) Kamiyama, A.; Noguchi, T.; Kajiwara, T.; Ito, T. *Inorg. Chem.* **2002**, *41*, 507. (c) Kajiwara, T.; Nakano, M.; Kaneko, Y.; Takaishi, S.; Ito, T.; Yamashita, M.; Igashira-Kamiyama, A.; Nojiri, H.; Ono, Y.; Kojima, N. *J. Am. Chem. Soc.* **2005**, *127*, 10150. (d) Kajiwara, T.; Sensui, R.; Noguchi, T.; Kamiyama, A.; Ito, T. *Inorg. Chim. Acta* **2002**, *337*, 299. (e) Kamiyama, A.; Noguchi, T.; Kajiwara, T.; Ito, T. *Angew. Chem., Int. Ed.* **2000**, *39*, 3130. (f) Kajiwara, T.; Ito, T. *J. Chem. Soc., Dalton Trans.* **1998**, 3351.

 Published on Web 10/23/2009

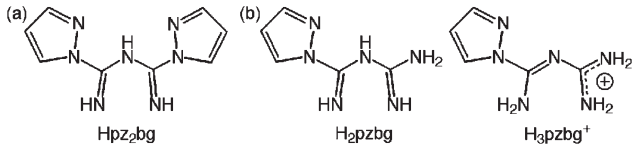

Figure 1. Drawing of the ligands, Hpz_2bg (a) and H_2pzbg (b).

Scheme 1. Synthesis of H_3pzbg^+ (top) and Coordination Modes of $pzbg^{2-}$ and $Hpzbg^-$ (bottom)

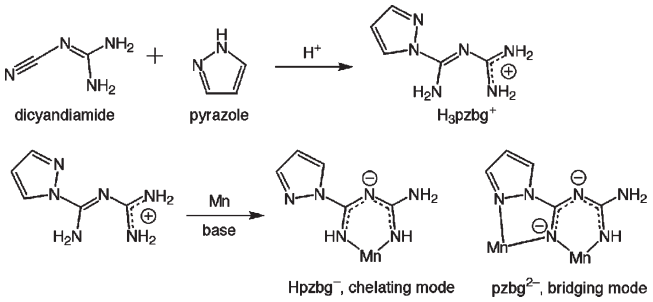

complex ligand $[Cu(pz_2bg)_2]$ is useful for producing ferromagnetic coupling. However, the organic ligand Hpz_2bg is unstable to be isolated, and a similar mononuclear metal complex including a metal ion other than Cu(II) has not been obtained. Therefore, we have now synthesized a similar ligand, H_3pzbg^+ (H_2pzbg is a monopyrazolyl derivative of biguanide, Figure 1b), that might bridge metal ions with a $\kappa^1N{:}\kappa^2N$ manner. Contrary to our expectation, the H_3pzbg^+ ligand was found to adopt different and more complicated coordination modes by using four nitrogen donors with different coordination manners. Here we report the syntheses and structures of this novel multinucleating ligand H_3pzbg^+ and its Mn(III) complexes, $[Mn(III)_4(\mu\text{-pzbg})_2(Hpzbg)_2(MeO)_4(MeOH)(H_2O)]Cl_2$ (**1**) and $[Mn(III)_6O_4(Hpzbg)_4(AcO)_4(MeO)_2]$ (**2**). As described below, **1** has an incomplete face-sharing double-cubane structure, in which H_3pzbg^+ shows two types of coordination modes by deprotonation (Scheme 1); one is a chelating mode (κ^2N-$Hpzbg^-$), and the other is a novel bridging mode ($\kappa^2N{:}\kappa^2N$-$pzbg^{2-}$). Interestingly, a ferromagnetic interaction occurs between Mn(III) ions through the imino nitrogen atom in **1**. On the other hand, **2** was found to have a face-sharing double-cubane structure with chelating κ^2N-$Hpzbg^-$. The magnetic property of **2** is also described.

Experimental Section

All solvents and chemicals were purchased as reagent grade and used without further purification. Fourier transform infrared spectroscopy was performed on a JASCO FT/IR-620 instrument as KBr pellets. Variable-temperature magnetic susceptibility measurements were made using a SQUID magnetometer MPMS 5S (Quantum Design) at 0.2 T for **1** and 1 T for **2**, respectively. Diamagnetic correction for each sample was determined from Pascal's constants.

Synthesis of $H_3pzbgCl\cdot H_2O$. To a solution containing pyrazole (410 mg, 6 mmol) in water (1.5 mL) was added conc. HCl (600 mg, 6 mmol) and dicyandiamide (510 mg, 6 mmol), which was stirred at 80 °C for 30 min. The resulting colorless solution was cooled to room temperature slowly, and colorless crystals of $H_3pzbgCl\cdot H_2O$ that appeared were filtered and dried in the air (625 mg, 3 mmol, 50%). Anal. Calcd for $C_5H_{11}ClN_6O$ ($H_3pzbgCl\cdot H_2O$): C, 29.06; H, 5.37; N, 40.67. Found: C, 29.04; H, 5.36; N, 40.70. IR (KBr disk, cm^{-1}): ν(CN) 1646 (s).

Synthesis of $[Mn(III)_4(pzbg)_2(Hpzbg)_2(MeO)_4(MeOH)(H_2O)]Cl_2\cdot 3MeOH\cdot H_2O$(1·3MeOH·H2O). To a solution containing $H_3pzbgCl\cdot H_2O$ (20 mg, 0.1 mmol) in MeOH (3 mL) was added a solution of $Mn(NO_3)_2\cdot 6H_2O$ (29 mg, 0.1 mmol) in MeOH (1 mL), followed by the addition of a solution of Et_3N (20 mg, 0.2 mmol) in MeOH (2 mL). The resulting orange solution was left at room temperature overnight, during which time the solution color changed to dark orange. Dark orange plate crystals of $\mathbf{1}\cdot 3MeOH\cdot H_2O$ were formed by slow evaporation at room temperature, which were collected and dried in the air (23 mg, 0.022 mmol, 87%). Anal. Calcd for $C_{25}H_{46}Cl_2Mn_4N_{24}O_7$ ($\mathbf{1}\cdot H_2O$): C, 27.66; H, 4.27; N, 30.97. Found: C, 27.55; H, 4.15; N, 30.72. IR (KBr disk, cm^{-1}): ν(CN) 1589 (s).

Synthesis of $[Mn(III)_6O_4(Hpzbg)_4(AcO)_4(MeO)_2]\cdot 2MeOH\cdot 4H_2O$(2·2MeOH·4H2O). To a solution containing $H_3pzbgCl\cdot H_2O$ (20 mg, 0.1 mmol) in MeOH (3 mL) was added a solution of $Mn(AcO)_2\cdot 4H_2O$ (25 mg, 0.1 mmol) in MeOH (1 mL), followed by the addition of a solution of Et_3N (20 mg, 0.2 mmol) in MeOH (2 mL). The resulting orange solution was left at room temperature overnight, during which time the solution color changed to dark orange. Dark orange plate crystals of $\mathbf{2}\cdot 2MeOH\cdot 4H_2O$ were formed by slow evaporation at room temperature, which were collected and dried in the air (22 mg, 0.017 mmol, 68%). Anal. Calcd for $C_{30}H_{52}Mn_6N_{24}O_{17}$ ($\mathbf{2}\cdot 3H_2O$): C, 26.68; H, 3.88; N, 24.89. Found: C, 26.52; H, 4.02; N, 24.50. IR (KBr disk, cm^{-1}): ν(CN) 1614 (s).

Crystal Structure Analyses. X-ray data for all complexes were collected at low temperature (200 and 243 K) with a Bruker SMART APEX diffractometer using graphite monochromated Mo Kα radiation (λ = 0.71073 Å). The data integration and reduction were undertaken with SAINT and XPREP.[10] An empirical correction for absorption was applied using the program SADABS.[11] The structures were solved by direct methods using SIR97[12] or SHELXS-97,[13] and the structure refinements were carried out using full-matrix least-squares (SHELXL-97[14]). For $H_3pzbgCl\cdot H_2O$, all non-hydrogen atoms were refined anisotropically, while hydrogen atoms were located from the difference Fourier map and refined isotropically. For $\mathbf{1}\cdot 3MeOH\cdot H_2O$, all non-hydrogen atoms except for disordered atoms were refined anisotropically, while the other atoms were refined isotropically. Hydrogen atoms were included in calculated positions except those of water and MeOH molecules. For $\mathbf{2}\cdot 2MeOH\cdot 4H_2O$, all non-hydrogen atoms were refined anisotropically, while hydrogen atoms were included in calculated positions except for those of water and MeOH molecules. A summary of the crystallographic data and structure determination parameters is provided in Table 1. CCDC-735765 ($H_3pzbgCl\cdot H_2O$), CCDC-735766 ($\mathbf{1}\cdot 3MeOH\cdot H_2O$), and CCDC-735767 ($\mathbf{2}\cdot 2MeOH\cdot 4H_2O$) contain the supplementary crystallographic data for this paper.

Results and Discussion

Syntheses. The synthesis of $H_3pzbgCl\cdot H_2O$ was performed by the nucleophilic addition of a secondary amine (pyrazole, Hpz) to a cyano group of dicyandiamide in the

(10) *SMART, SAINT, and XPREP, Area detector control and data integration and reduction software*; Bruker Analytical X-ray Instruments Inc.: Madison, WI, 1995.
(11) Sheldrick, G. M. *SADABS, Empirical absorption correction program for area detector data*; University of Göttingen: Göttingen, Germany, 1996.
(12) Altomare, A.; Burla, M. C.; Camalli, M.; Cascarano, G. L.; Giacovazzo, C.; Guagliardi, A.; Moliterni, A. G. G.; Polidori, G.; Spagna, R. *J. Appl. Crystallogr.* **1999**, *32*, 115–119.
(13) Sheldrick, G. M. *SHELXS97, Program for Structure Solution*; University of Göttingen: Göttingen, Germany, 1997.
(14) Sheldrick, G. M. *SHELXL97, Program for the Refinement of Crystal Structures*; University of Göttingen, Göttingen, Germany, 1997.

Table 1. Crystallographic Data for $H_3pzbgCl\cdot H_2O$, $1\cdot 3MeOH\cdot H_2O$, and $2\cdot 2MeOH\cdot 4H_2O$

	$H_3pzbgCl\cdot H_2O$	$1\cdot 3MeOH\cdot H_2O$	$2\cdot 2MeOH\cdot 4H_2O$
formula	$C_5H_{11}ClN_6O$	$C_{28}H_{58}Cl_2Mn_4N_{24}O_{10}$	$C_{32}H_{62}Mn_6N_{24}O_{20}$
fw	206.65	1181.64	1432.70
crystal system	monoclinic	monoclinic	monoclinic
space group	$P2_1/c$	$P2_1/n$	$C2/m$
a [Å]	12.4347(16)	10.5683(12)	12.348(2)
b [Å]	5.2803(7)	21.205(2)	24.911(5)
c [Å]	14.927(2)	11.5868(13)	9.7567(18)
β [°]	104.904(3)	104.614(3)	108.533(4)
V [Å^3]	947.2(2)	2512.6(5)	2845.6(9)
Z	4	2	2
T [K]	243(2)	223(2)	223(2)
ρ_{calcd} [g cm^{-3}]	1.449	1.562	1.672
μ [mm^{-1}]	0.377	1.161	1.381
$R1$ [$I > 2\sigma(I)$][a]	0.0444	0.0680	0.0637
w$R2$ [$I > 2\sigma(I)$][b]	0.1083	0.1776	0.1186
$R1$ [all data][a]	0.0504	0.1626	0.1332
w$R2$ [all data][b]	0.1115	0.2073	0.1384

[a] $R1 = \sum||F_o| - |F_c||/\sum|F_o|$. [b] $wR2 = [\sum w(F_o^2 - F_c^2)^2/\sum w(F_o^2)^2]^{1/2}$.

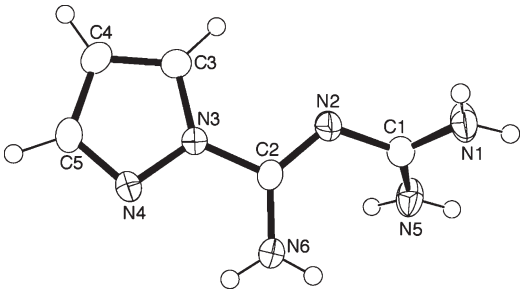

Figure 2. ORTEP drawings of H_3pzbg^+ with thermal ellipsoids at 50% probability.

presence of acid (Scheme 1).[7,15] While the nucleophilic additions in basic condition have been also reported,[16] a similar reaction using NaOH instead of HCl gave only unidentified mixtures. Compound $H_3pzbgCl\cdot H_2O$ contains five nitrogen atoms that can coordinate to metal ions after continuous deprotonations. The reactions of $H_3pzbgCl\cdot H_2O$ with Mn(II) salts in the presence of Et_3N afforded tetramanganese(III) (**1**) and hexamanganese(III) (**2**) complexes, depending on the counteranion of the Mn(II) sources, that is, **1** was obtained when $Mn(NO_3)_2\cdot 6H_2O$ was used, whereas **2** was obtained on using $Mn(AcO)_2\cdot 4H_2O$. It was found that the reaction ratio of the Mn(II) salt to $H_3pzbgCl\cdot H_2O$ does not affect the formation of final products. The amount of Et_3N also did not affect the formation of the polymanganese(III) structures, although the ligand in each complex adopts different deprotonated forms (vide infra).

Structures. Structure of $H_3pzbgCl\cdot H_2O$. The structure of the cationic part of $H_3pzbgCl\cdot H_2O$ is shown in Figure 2, and its selected atom−atom distances are listed in Table 2. A nitrogen atom of pyrazole (N3) is bound to carbon atom (C2) of a cyano group of dicyandiamide, producing H_3pzbg^+ as a protonated form. The C2—N2 bond distance (1.2939(19) Å) shows a double bond character (Scheme 1), and the positive charge delocalizes over the N1—C1—N5 moiety, which is indicated by the bond distances (N—C = 1.316(2), 1.318(2) Å). The N1, N2, N5, and C1 atoms are coplanar, and the pyrazolyl ring and the N2, C2, and N6 atoms are also coplanar. The dihedral angle of these two planes is approximately 60°.

Table 2. Selected Distances [Å] for $H_3pzbgCl\cdot H_2O$

N1—C1	1.316(2)	N2—C2	1.2939(19)
N2—C1	1.356(2)	N3—C2	1.4005(18)
N5—C1	1.318(2)	N6—C2	1.321(2)

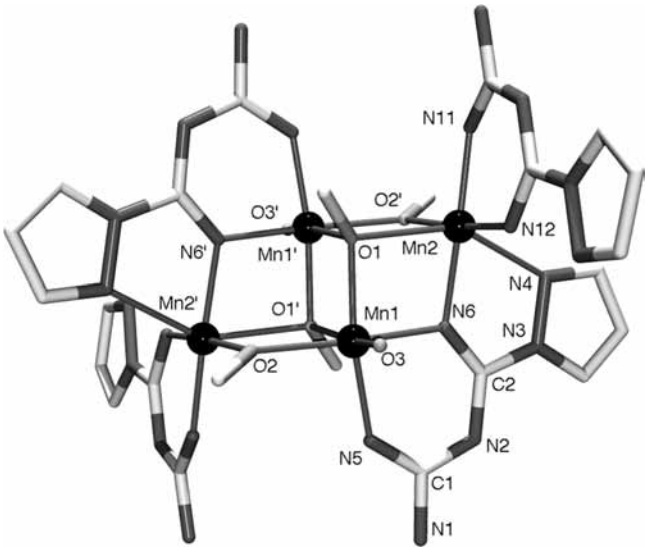

Figure 3. Crystal structure of the cationic part of **1**. Hydrogen and disordered carbon atoms are omitted for clarity. Each atom is depicted as follows: Mn black sphere, N gray, O light-gray, C white. Symmetry codes: (′) $-x + 2, -y, -z + 1$.

Structure of $[Mn(III)_4(pzbg)_2(Hpzbg)_2(MeO)_4(MeOH)(H_2O)]Cl_2\cdot 3MeOH\cdot H_2O$ ($1\cdot 3MeOH\cdot H_2O$). The structure of **1** possesses an incomplete face-sharing double cubane core, as shown in Figure 3 and Table 3. The asymmetric unit contains a half of the entire molecule, and a crystallographic inversion center is located at the center of the core. The cluster core consists of four manganese ions, two nitrogen atoms from two $pzbg^{2-}$,

(15) (a) Cohn, G. *J. Prakt. Chem.* **1911**, *84*, 394. (b) Rembarz, G.; Brandner, H.; Finger, H. *J. Prakt. Chem.* **1964**, *26*, 314. (c) Khripun, A. V.; Kukushkin, V. Y.; Selivanov, S. I.; Haukka, M.; Pombeiro, A. J. L. *Inorg. Chem.* **2006**, *45*, 5073.

(16) Boa, R.; Hvastijová, M.; Koíek, J.; Valko, M. *Inorg. Chem.* **1996**, *35*, 4794.

Table 3. Selected Distances [Å] and Angles [deg] for $1 \cdot 3MeOH \cdot H_2O$[a]

Mn1—N5	1.931(5)	Mn1—N6	1.910(5)
Mn1—O1	1.958(4)	Mn1—O2	1.965(4)
Mn1—O3	2.229(5)	Mn1—O1′	2.276(4)
Mn2—N4	2.297(6)	Mn2—N6	1.972(5)
Mn2—N11	1.939(5)	Mn2—N12	1.931(6)
Mn2—O1	2.231(4)	Mn2—O2′	1.953(4)
Mn1···Mn2	3.1155(14)	Mn1···Mn1′	3.231(2)
N1—C1	1.336(8)	N2—C1	1.318(9)
N2—C2	1.316(7)	N3—C2	1.408(8)
N7—C6	1.330(8)	N8—C6	1.345(9)
N8—C7	1.310(8)	N9—C7	1.384(8)
N11—C6	1.333(8)	N12—C7	1.314(7)
Mn1—N6—Mn2	106.8(2)	Mn1—O1—Mn1′	99.22(15)
Mn1—O1—Mn2	95.87(15)	Mn2—O1—Mn1′	92.02(4)
Mn1—O2—Mn2′	111.5(2)		

[a] Symmetry code: (′) $-x+2, -y, -z+1$.

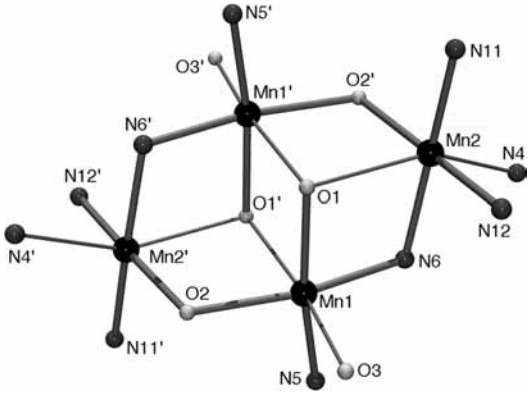

Figure 4. Incomplete face-sharing double cubane core of **1**. Each atom is depicted as follows: Mn black sphere, N gray, O light-gray. Symmetry codes: (′) $-x+2, -y, -z+1$.

and four MeO^- oxygen atoms (Figure 4). The oxidation state of each manganese ion is estimated to be +3 based on the charge balance of the formula. In addition, the bond valence sum (BVS) values calculated for Mn1 and Mn2 are 3.26 and 3.36, respectively,[17] which are close to the expected value of 3.00 for Mn(III). Each Mn(III) ion is in an axially elongated octahedral geometry, typical for a high spin Mn(III) ion. The thick and thin bonds in Figure 4 represent the equatorial and axial (Jahn−Teller axis) bonds, respectively. The Mn1 atom is surrounded by two nitrogen atoms from $pzbg^{2-}$ (N5 and N6) and two oxygen atoms from MeO^- ions (O1 and O2) in an equatorial plane (Mn—N = 1.931(5) and 1.910(5) Å, Mn—O = 1.958(4) and 1.965(4) Å) and two oxygen atoms from a MeO^- ion (O1′) and a water molecule (O3) in axial positions (Mn—O = 2.276(4) and 2.229(5) Å). The Mn2 atom is surrounded by three nitrogen atoms from $pzbg^{2-}$ (N6) and $Hpzbg^-$ (N11 and N12) and one oxygen atom from a MeO^- ion (O2′) in an equatorial plane (Mn—N = 1.931(6)−1.972(5) Å, Mn—O = 1.953(4) Å), while a nitrogen atom from $pzbg^{2-}$ (N4) and an oxygen atom from a MeO^- ion (O1) occupy axial positions (Mn—N = 2.297(6) Å and Mn—O = 2.231(4) Å). The H_2pzbg ligands in **1** show two different coordination fashions; one is terminating monoanionic ($Hpzbg^-$) and the other is bridging dianionic ($pzbg^{2-}$) (Scheme 1). The former coordinates to Mn2 via two $N_{C=NH}$ nitrogen atoms as a

(17) Brown, I. D.; Altermatt, D. *Acta Crystallogr.* **1985**, *B41*, 244.

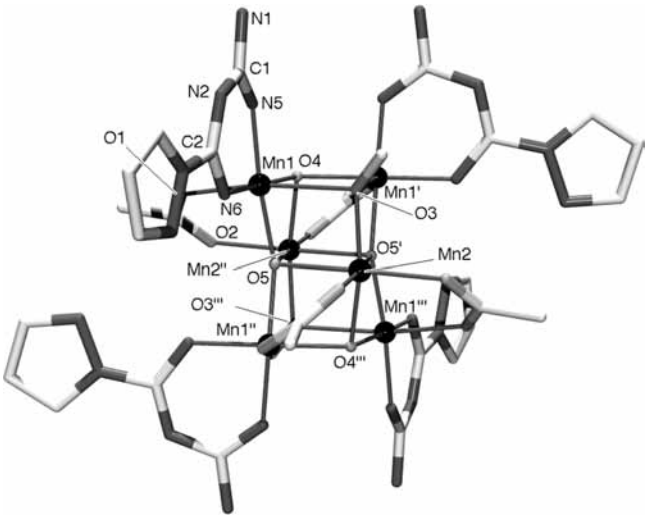

Figure 5. Crystal structure of **2**. Hydrogen atoms are omitted for clarity. Each atom is depicted as follows: Mn black sphere, N gray, O light-gray, C white. Symmetry codes: (′) $-x, -y, -z+1$, (″) $x, -y, z$, (‴) $-x, y, -z+1$.

chelating ligand, and the negative charge delocalizes on the entire N—C—N—C—N conjugated system, which is indicated by the uniformity of the N—C distances (1.310(8)−1.345(9) Å). A further deprotonation from an imino nitrogen $N_{C=NH}$ (N6) of $Hpzbg^-$ gives $pzbg^{2-}$ that bridges Mn1 and Mn2 through the anionic imino nitrogen $N_{C=N}-$ (N6). The C—N distances of $pzbg^{2-}$ indicate that the negative charge localizes over the conjugated system (C—N = 1.287(7)−1.335(8) Å). Only a few Werner-type complexes with a bridging imino nitrogen have been reported previously,[18] and the bridging mode found here is uncommon. This peculiar coordination would be achieved by the stabilization due to the π-system spreading over the whole structure of the ligand as well as the chelating effect. Similar tetra-manganese complexes having a Mn_4O_6 incomplete double cubane core were commonly known; however, most of them were the mixed valent $Mn(II)_2Mn(III)_2$ species.[19] Only two $Mn(III)_4$ complexes were reported, in which the relative orientation of the Jahn−Teller axes is different from that in **1**.[20]

Structure of $[Mn(III)_6O_4(Hpzbg)_4(AcO)_4(MeO)_2] \cdot 2MeOH \cdot 4H_2O$ ($2 \cdot 2MeOH \cdot 4H_2O$). The structure of **2** involves a face-sharing double cubane core, as shown in Figure 5 and Table 4. The asymmetric unit contains a quarter of the entire molecule, and a crystallographic inversion center is located at the center of the molecule, with a mirror plane including the Mn2, Mn2′, O3, O3′,

(18) (a) Soloshonok, V. A.; Ueki, H. *J. Am. Chem. Soc.* **2007**, *129*, 2426. (b) Fomina, I. G.; Sidorov, A. A.; Aleksandrov, G. G.; Nefedov, S. E.; Eremenko, I. L.; Moiseev, I. I. *J. Organomet. Chem.* **2001**, *636*, 157. (c) Davies, M. K.; Raithby, P. R.; Rennie, M.-A.; Steiner, A.; Wright, D. S. *J. Chem. Soc., Dalton Trans.* **1995**, 2707.

(19) (a) Wittick, L. M.; Jones, L. F.; Jensen, P.; Moubaraki, B.; Spiccia, L.; Berry, K. J.; Murray, K. S. *Dalton Trans.* **2006**, 1534. (b) Wittick, L. M.; Murray, K. S.; Moubaraki, B.; Batten, S. R.; Spiccia, L.; Berry, K. J. *Dalton Trans.* **2004**, 1003. (c) Yoo, J.; Brechin, E. K.; Yamaguchi, A.; Nakano, M.; Huffman, J. C.; Maniero, A. L.; Brunel, L.-C.; Awaga, K.; Ishimoto, H.; Christou, G.; Hendrickson, D. N. *Inorg. Chem.* **2000**, *39*, 3615. (d) Yang, E.-C.; Harden, N.; Wernsdorfer, W.; Zakharov, L.; Brechin, E. K.; Rheingold, A. L; Christou, G.; Hendrickson, D. N. *Polyhedron* **2003**, *22*, 1857.

(20) (a) Mikuriya, M.; Yamato, Y.; Tokii, T. *Bull. Chem. Soc. Jpn.* **1992**, *65*, 2624. (b) Mikuriya, M.; Nakadera, K.; Kotera, T.; Tokii, T.; Mori, W. *Bull. Chem. Soc. Jpn.* **1995**, *68*, 3077.

Table 4. Selected Distances [Å] and Angles [deg] for $2 \cdot 2MeOH \cdot 4H_2O$[a]

Mn1—N5	1.941(4)	Mn1—N6	1.944(4)
Mn1—O1	2.187(4)	Mn1—O3	2.358(3)
Mn1—O4	1.939(2)	Mn1—O5	1.9190(10)
Mn2—O2′	2.041(4)	Mn2—O2‴	2.041(4)
Mn2—O3	1.903(4)	Mn2—O4′	1.911(4)
Mn2—O5′	2.148(3)	Mn2—O5	2.148(3)
N1—C1	1.345(7)	N2—C1	1.345(7)
N2—C2	1.311(7)	N3—C2	1.405(7)
N5—C1	1.318(6)	N6—C2	1.311(7)
Mn1···Mn2	3.1422(13)	Mn1···Mn1″	3.2430(16)
Mn1···Mn2′	2.8655(11)		
Mn1—O3—Mn1″	86.89(15)	Mn1—O3—Mn2	94.43(14)
Mn1—O4—Mn1″	113.5(2)	Mn1—O4—Mn2′	96.19(15)
Mn1—O5—Mn1‴	163.4(3)	Mn1—O5—Mn2	101.03(9)
Mn1—O5—Mn2′	89.41(8)	Mn2—O5—Mn2′	102.53(19)

[a] Symmetry codes: (′) $-x, -y, -z+1$, (″) $x, -y, z$, (‴) $-x, y, -z+1$.

O4, and O4′ atoms and a 2-fold axis passing along the O5—O5′ vector. The double cubane core consists of six manganese ions, two μ_4-oxygen (O5), two μ_3-oxygen (O4), and two μ_3-oxygen (O3, MeO^-) atoms, besides four bridging acetates that stabilize the double cubane core. The oxidation number of each Mn atom (Mn(II), Mn(III), or Mn(IV)) and protonation/deprotonation of μ_4-O5 and μ_3-O4 (OH^- or O^{2-}) were determined by the geometrical considerations as well as BVS calculations for manganese ions, in combination with the charge balance. The BVS values calculated for Mn1 and Mn2 are 3.26 and 2.98, respectively, which are in agreement with the expected value of 3.00 for Mn(III). Considering the trivalent state of Mn1 and Mn2, both the μ_4-O5 and the μ_3-O4 atoms are determined to be O^{2-}. The Mn1 ion is in an axially elongated octahedral geometry surrounded by two nitrogen atoms from $Hpzbg^-$ (N5 and N6) and two oxygen atoms from O^{2-} ions (O4 and O5) in an equatorial plane (Mn—N = 1.941(4) and 1.944(4) Å, Mn—O = 1.939(2) and 1.9190(10) Å) and two oxygen atoms from MeO^- ion (O3) and acetate ion (O1) in axial positions (Mn—O = 2.358(3) and 2.187(4) Å). The Mn2 atom is in a distorted octahedron surrounded by six oxygen atoms from two acetates (O2′ and O2‴), two μ_4-O^{2-} (O5 and O5′), one μ_3-O^{2-} (O4′), and one μ_3-MeO^- ion (O3) (Mn—O = 1.903(4)−2.148(3) Å). The Mn1 atom displays a typical Jahn−Teller elongation, whereas the situation for Mn2 is slightly complicated. Two oxygen atoms around Mn2 (O5 and O5′) with the relatively long distances are in a cis position, that is, Mn2 shows an disordered Jahn−Teller distortion. Four biguanidate ligands that take a monoanionic form ($Hpzbg^-$) behave equivalently as a chelating ligand. The negative charge of $Hpzbg^-$ delocalizes on the N—C—N—C—N conjugated system, similar to that found in **1** (C—N = 1.311(7)−1.345(7) Å). To our knowledge, only one hexamanganese complex having a face-sharing double cubane structure was reported previously,[21] and **2** is a second example.

Magnetic Properties. The temperature dependent magnetic susceptibilities of **1** and **2** were measured down to 2 K. Figure 6 shows the magnetic data for **1**. The $\chi_M T$ value of 12.20 cm^3 K mol^{-1} at room temperature is slightly larger than the spin only value of 12.0 cm^3 K mol^{-1} for four Mn(III) ions with a g value of 2.0. On lowering the temperature, the $\chi_M T$ values gradually increase, reaching 15.53 cm^3 K mol^{-1} at 44 K, which suggests the presence of a ferromagnetic interaction in **1**. Then, the $\chi_M T$ values decrease to 9.12 cm^3 K mol^{-1} at 2 K, indicating the presence of intramolecular and intermolecular antiferromagnetic interactions between the Mn(III) ions as well as the zero-field splitting of the Mn(III) ions. From the consideration of the molecular structure, three exchange parameters would be needed to describe the magnetic behavior of **1** (Scheme 2) with the corresponding Hamiltonian of

$$H = -2J_1(S_{Mn1} \cdot S_{Mn2} + S_{Mn3} \cdot S_{Mn4}) - 2J_2(S_{Mn1} \cdot S_{Mn4} + S_{Mn2} \cdot S_{Mn3}) - 2J_3 S_{Mn1} \cdot S_{Mn3}$$

where J_1 and J_2 denote the interactions between terminal and central Mn(III) ions and J_3 is for the central Mn(III) ions.[22] As a beginning, we considered a butterfly type model ($J_1 = J_2$), but this failed to explain the temperature dependence of magnetism of **1**. Therefore, we assumed that the J_1 and J_2 should be independent, and the calculations were performed with four parameters (g, J_1, J_2, and J_3) using the data above 20 K to avoid the influence of the intermolecular interaction as well as the zero-field splitting of the Mn(III) ions. The final parameters were evaluated as $g = 1.86$, $J_1 = -0.3$ cm^{-1}, $J_2 = +9.4$ cm^{-1}, and $J_3 = -0.1$ cm^{-1} with $R = 0.0031$, after the calculations with the several sets of the initial values.[23] The result here is different from those of $Mn(III)_4$ complexes, for which only antiferromagnetic interactions were observed among Mn(III) ions.[20] From the fitting parameters, it is shown that the spin ground state is $S = 0$ with several excited states close to the ground state (Figure S1, Supporting Information). The field dependent

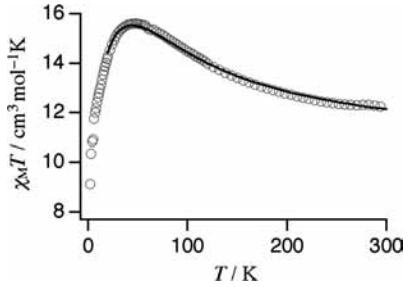

Figure 6. Plots of $\chi_M T$ vs T for **1**. Solid line corresponds to the theoretical curve for which parameters are given in the text.

Scheme 2. Core Structure of **1** in which Gray and Black Arrows Represent the Pathways A and B, Respectively (a), and a Schematic Drawing of J_1, J_2, and J_3 (b)

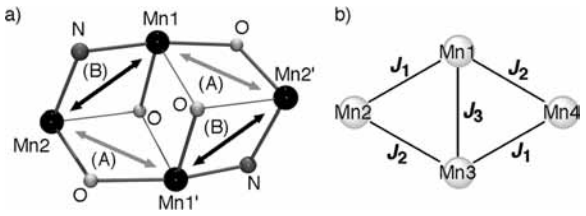

(21) Godbole, M. D.; Roubeau, O.; Mills, A. M.; Kooijman, H.; Spek, A. L.; Bouwman, E. *Inorg. Chem.* **2006**, *45*, 6713.

(22) Kahn, O. *Molecular Magnetism*; VCH: New York, 1993.

(23) The several attempts of the fitting lead to the J_1 and J_3 values between -1 cm^{-1} and $+1$ cm^{-1} depending on the initial values, but final parameters were determined based on the R value.

magnetization does not show the saturation up to 5 T at 2 K, which may be due to the magnetic anisotropy of the excited states close to the ground state (Figure S2, Supporting Information). As was predicted from the spin ground state, **1** does not show the single molecule magnet behavior in the ac magnetic susceptibility measurement.

In the tetra-manganese(III) core in **1**, a relatively strong ferromagnetic interaction (J_2) and weak antiferromagnetic interactions (J_1 and J_3) coexist. J_3 uniquely corresponds to the interaction between the central Mn(III) ions. For J_1 and J_2, there are two corresponding pathways between the central and terminal Mn(III) ions such as a pathway through two MeO^- oxygen atoms (pathway A) and through bridging imino nitrogen and MeO^- oxygen atoms (pathway B). It is difficult to determine the parameters J_1/J_2 to be corresponding to the pathways A/B or pathways B/A from the analysis given above, and an acceptable assignment was achieved by the comparison with the magnetic data for the reported complexes. The magnetic interaction between Mn(III) ions depends both on the relative orientation of the Jahn−Teller axes and on the bridging angles. When the Mn—O—Mn moiety comprises one equatorial and one axial bond from elongated octahedrons, a ferromagnetic interaction can be observed through the crossed interaction between singly occupied (d_{z^2}) and empty ($d_{x^2-y^2}$) orbitals with the bridging angle of ∼120° or through the orthogonality of the magnetic orbitals (d_{z^2} and $d\pi$) with the bridging angle at ∼100°. On the other hand, antiferromagnetic couplings dominate for the other combinations of Jahn−Teller axes in any bonding angles.[24−26] In the case of pathway A, two oxygen bridged Mn—O—Mn moieties comprise two equatorial (Mn1—O2—Mn2′) and two axial (Mn1—O1′—Mn2′) bonds, respectively, and antiferromagnetic interactions would be predicted. In the pathway B, the Mn1—N6—Mn2 moiety consists of two equatorial bonds, and the Mn1—O1—Mn2 moiety includes one equatorial and one axial bond, which can produce both ferromagnetic and antiferromagnetic interactions. Although the magnetic interaction via imino nitrogen has not been reported so far, this interaction was compared with that via a $\mu_{1,1}$-azide nitrogen atom as a good reference, which showed the presence of a ferromagnetic interaction between Mn(III) ions.[27] From these considerations, we concluded that the interaction via pathway A is antiferromagnetic (J_1) and the interaction through pathway B is ferromagnetic (J_2).

Figure 7 shows the magnetic data for **2**. The $\chi_M T$ value at 300 K is 11.13 cm^3 K mol^{-1}, which is much smaller than the spin only value of 18.0 cm^3 K mol^{-1} for six Mn(III) ions with the g value of 2.0. The $\chi_M T$ value

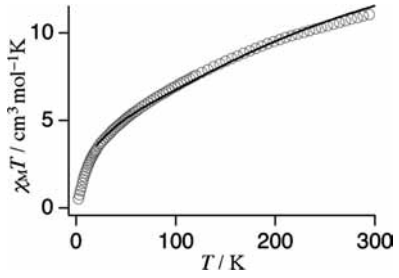

Figure 7. Plots of $\chi_M T$ vs T for **2**. Solid line corresponds to the theoretical curve for which parameters are given in ref 28.

gradually decreases as the temperature goes down, indicative of the presence of a strong antiferrromagnetic coupling between the Mn(III) ions,[28] which is predominant even at room temperature. The magnetic data obeys the Curie−Weiss law in a high temperature region, and fitting in the range 90−300 K gives a negative Weiss constant (C = 15.78(8) cm^3 K mol^{-1} and $\theta = -129(2)$ K). The spin ground state of **2** is $S = 0$, as indicated by the field dependent magnetization, which shows small values up to 5 T at 2 K (Figure S3, Supporting Information).

Conclusion

We succeeded in the synthesis of a novel multinucleating ligand, H_3pzbg^+, which can possess up to four coordination sites (including five nitrogen atoms) accompanied by deprotonation. The reactions of H_3pzbg^+ and Mn(II) ion in the presence of base afforded the incomplete double cubane tetramanganese(III) complex (**1**) and the double cubane hexamanganese(III) complex (**2**), depending on the counteranions of the Mn(II) sources. The monoanionic $Hpzbg^-$ behaves as a chelating ligand via two imide nitrogen atoms ($N_{C=NH}$), while the dianionic $pzbg^{2-}$ adopts a bridging mode through an imino nitrogen atom ($N_{C=N^-}$), which is an unusual bridging mode.[18] There exists both ferromagnetic and antiferromagnetic interactions between Mn(III) ions in **1**, whereas a strong antiferromagnetic interaction occurs in **2**. The magnetic interaction via an imino nitrogen has not been reported yet, and complex **1** is the first example. It is noteworthy that the magnetic interaction between Mn(III) ions via an imino nitrogen is assigned to be ferromagnetic. Thus, the use of an imino nitrogen as a bridging atom would be useful for the construction of polynuclear complexes bearing a large ground spin state.

Acknowledgment. This work was supported by Grants-in-Aid for Young Scientists B (No. 20750047) from Japan Society for the Promotion of Science, Japan, as well as by JSPS Research Fellowships for Young Scientists (No. 12006281).

Supporting Information Available: X-ray crystallographic files in CIF format and magnetic data. This material is available free of charge via the Internet at http://pubs.acs.org.

(24) (a) Hotzelmann, R.; Wieghardt, K.; Flörke, U.; Haupt, H.-J.; Weatherburn, D. C.; Bonvoisin, J.; Blondin, G.; Girerd, J.-J. *J. Am. Chem. Soc.* **1992**, *114*, 1681. (b) Caneschi, A.; Gatteschi, D.; Sessoli, R. *J. Chem. Soc., Dalton Trans.* **1997**, 3963. (c) Abbati, G. L.; Cornia, A.; Fabretti, A. C.; Caneschi, A.; Gatteschi, D. *Inorg. Chem.* **1998**, *37*, 1430.

(25) (a) Miyasaka, H.; Clérac, R.; Ishii, T.; Chang, H.-C.; Kitagawa, S.; Yamashita, M. *J. Chem. Soc., Dalton Trans.* **2002**, 1528. (b) Miyasaka, H.; Clérac, R. *Bull. Chem. Soc. Jpn.* **2005**, *78*, 1725.

(26) (a) Zhang, Z.-Y.; B.-Cabarrecq, C.; Hemmert, C.; Dahan, F.; Tuchagues, J.-P. *J. Chem. Soc., Dalton Trans.* **1995**, 1453. (b) Vincent, J. B.; Christmas, C.; Chang, H.-R.; Li, Q.; Boyd, P. D. W.; Huffman, J. C.; Hendrickson, D. N.; Christou, G. *J. Am. Chem. Soc.* **1989**, *111*, 2086.

(27) Ge, C.-H.; Cui, A.-L.; Ni, Z.-H.; Jiang, Y.-B.; Zhang, L.-F.; Ribas, J.; Kou, H.-Z. *Inorg. Chem.* **2006**, *45*, 4883.

(28) Observed data were well reproduced when five magnetic pathways were assumed on the basis of the Hamiltonian, $H = -2J_1(S_{Mn1}\cdot S_{Mn1'} + S_{Mn1''}\cdot S_{Mn1'''}) - 2J_2(S_{Mn1}\cdot S_{Mn2''} + S_{Mn1'}\cdot S_{Mn2''} + S_{Mn2}\cdot S_{Mn1''} + S_{Mn2}\cdot S_{Mn1'''}) - 2J_3(S_{Mn1}\cdot S_{Mn2} + S_{Mn1'}\cdot S_{Mn2} + S_{Mn2''}\cdot S_{Mn1''} + S_{Mn2''}\cdot S_{Mn1'''}) - 2J_4(S_{Mn2}\cdot S_{Mn2''}) - 2J_5(S_{Mn1}\cdot S_{Mn2''} + S_{Mn1'}\cdot S_{Mn1'''})$, which gave the estimated J values of $J_1 = -4.7$ cm^{-1}, $J_2 = -1.0$ cm^{-1}, $J_3 = -2.4$ cm^{-1}, $J_4 = -2.6$ cm^{-1}, and $J_5 = -44$ cm^{-1}. Five parameters would be overparametric; however, attempts to fit with two or three averaged exchange parameters failed.